

The Irradiation of Water Ice by C^+ ions in the Cosmic Environment

E. J. McBride,^{†,‡} T. J. Millar,^{†,¶} and J. J. Kohanoff^{*,†,‡}

School of Mathematics and Physics, Queen's University Belfast, Belfast BT7 1NN, Northern Ireland, UK

E-mail: j.kohanoff@qub.ac.uk

*To whom correspondence should be addressed

[†]Queen's University Belfast

[‡]Atomistic Simulation Centre

[¶]Astrophysics Research Centre

Abstract

We present a first principles molecular dynamics (FPMD) study of the interaction of low energy, positively charged, carbon (C^+) projectiles with amorphous solid water clusters at 30 K. Reactions involving the carbon ion at an initial energy of 11 eV and 1.7 eV with 30-molecule clusters have been investigated. Simulations indicate that the neutral isoformyl radical, COH^\bullet , and carbon monoxide, CO, are the dominant products of these reactions. All these reactions are accompanied by the transfer of a proton from the reacting water molecule to the ice, where it forms a hydronium ion. We find that COH^\bullet is formed either via a direct, “knock-out”, mechanism following the impact of the C^+ projectile upon a water molecule or by creation of a COH_2^+ intermediate. The direct mechanism is more prominent at higher energies. CO is generally produced following the dissociation of COH^\bullet . More frequent production of the formyl radical, HCO^\bullet , is observed here than in gas phase calculations. A less commonly occurring product is the dihydroxymethyl, $CH(OH)_2^\bullet$, radical. Although a minor result, its existence gives an indication of the increasing chemical complexity which is possible in such heterogeneous environments.

Keywords: carbon, cluster, dynamics, ice, ion, water.

Introduction

Water ice is an important, often dominant, component of molecular ices in cold interstellar clouds, in bodies in the Solar System and, by extension, in extra-solar planets and proto-planetary disks. Such ices can experience non-thermal irradiation and interactions by UV and X-ray photons, particularly in the neighborhood of young stars, by cosmic-ray particles and high-energy ions and electrons. Particle acceleration can occur in shock fronts associated with supernovae explosions – see Dumas *et al.*¹ for a recent example of a supernovae remnant interacting with its surrounding molecular cloud –, in stellar flares, perhaps driven by episodic accretion in the formation of protostars, in Solar and stellar winds, and in planetary magnetospheres. It is thus of interest to

investigate the interaction of water ice with abundant atoms and atomic ions.

Ions are crucial to the chemistry of the interstellar medium (ISM).^{2,3} This is especially true in photon-dominated regions (PDRs) where interstellar gas is exposed to UV radiation from distant stars, leading to the formation of ionized species via photodissociation and photoionization. In these high-energy environments the carbon cation, C^+ , is predicted to be the most abundant ion.⁴

Carbon ions are also significant within our own solar system. Those found in planetary magnetospheres are believed to originate from the slow component of the solar wind⁵ while the Cassini Cosmic Dust analyzer has detected C^+ as a dominant component in the stream particles of Jupiter and Saturn.⁶

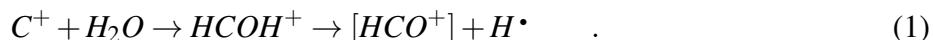
The reaction of C^+ with various small molecules has been the subject of much experimental and theoretical study.^{2,3,7-10} While the majority of previous work has focused on understanding gas-phase chemistry, here we investigate this reaction in the condensed phase, within the ice which is present on planetary bodies and which also envelopes the microscopic dust particles that are ubiquitous in the ISM.¹¹

In fact, heterogeneous reactions are believed to be important in the synthesis of complex molecules. Purely gas-phase routes to complex molecules have been shown to be inefficient while also failing to reproduce the observed abundances of some simpler species. It is thought that the modification and subsequent evaporation of ices in astrophysical environments by energetic particles may lead to the formation of larger organic species. One such example is the interaction of carbon ions with the icy surfaces present on Jupiter's Galilean moons. This reaction is evidenced by the detection of CO_2 on Callisto and Ganymede.¹²

Essentially the same phenomenon occurs upon C^{+q} irradiation of biological matter, when the ions gradually lose their energy to the medium along the radiation track, until their velocities are low enough that they can chemically react with water and other biomolecules. This happens just after the Bragg peak, at the end of the track, when ions have lost most of their kinetic energy and come close to rest.

Several studies have been undertaken to elucidate the mechanisms involved in reactions of C^+

with gas-phase water. Sonnenfroh *et al.*¹³ conducted one of the first experimental investigations of the $C^+ + H_2O$ reaction in the gas-phase, a crossed beam study with collision energies of 0.62 eV and 2.14 eV. They suggest that at the lower energy the production of either the formyl, HCO^+ , or isoformyl ion, COH^+ , occurs through the formation of a transient hydroxymethylene ion intermediate, $HCOH^+$. Subsequently, this complex decays via cleavage of the C-H bond to form the isoformyl cation COH^+ or by O-H bond cleavage to form the more stable formyl cation HCO^+ ,

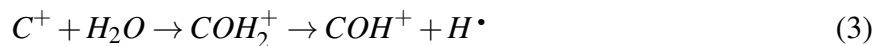


In 1 the notation $[HCO^+]$ denotes both the formyl and isoformyl ions. Sonnenfroh *et al.* reported that the formation of HCO^+ represents a significant fraction (20% – 30%) of the final products at the lower energy.

At the higher collision energy the fraction of HCO^+ produced is found to decrease. Sonnenfroh *et al.* proposed that this is the result of the increasing dominance of a direct, “knock-out” mechanism. In this alternative pathway the incoming C^+ cation strikes H_2O with an almost zero impact parameter causing the ejection of a hydrogen atom. The less stable isomer, COH^+ , is formed exclusively here. Their observations also suggest that at the lower collision energy approximately one third of the products have sufficient energy to surmount the HCO^+ / COH^+ isomerization barrier. At the higher collision energy this is the case for two thirds of the products.

Ishikawa *et al.*¹⁴ performed an ab initio QCISD/6-31+G* direct molecular dynamics (MD) study of the reaction of C^+ with water and the mechanism of reaction was examined. This work represented an attempt to approximate the low energy beam studies of Sonnenfroh *et al.*, the reactants here colliding with a relative kinetic energy of 0.62 eV. Their results have shown that the principal products are COH^+ and H^\bullet .





They have also shown that the two main channels in this reaction are by direct “knock-out” of a hydrogen (see 2) and via an intermediate, COH_2^+ (see 3). This intermediate is not one which has previously been proposed in either experimental or theoretical studies. Most of the isoformyl cations produced were found to be internally energetic enough to isomerize to the formyl cation.

The C^+ -water complex, COH_2^+ , was found to be the most common intermediate (see 1). This is at odds with the work of Sonnenfroh *et al.* who proposed that the hydroxymethylene intermediate, $HCOH^+$, should form. Ishikawa *et al.* suggested that the hydroxymethylene cation had been considered to be significant based on observations that C^+ undergoes bond insertion reactions.¹⁴ They stated, however, that these bond insertions had been with hydrocarbons which possess neither the polarity nor the convenient point of attachment presented by water.

Ishikawa *et al.* concluded that the collision of C^+ and H_2O at 0.62 eV produces COH^+ , with HCO^+ as a rare product of the immediate reaction. The great majority of HCO^+ must come via isomerization and most COH^+ possesses sufficient internal energy to isomerize. Their findings were substantiated by further study.¹⁵

Flores¹⁶ has presented a study of the $C^+ + H_2O \rightarrow COH^+ + H$ reaction in which the quasiclassical trajectory method has been employed. The electronic structure has been calculated using a B3LYP-type density functional approach while the potential energy surface has been represented via a finite element method. Trajectory computations have been performed at a fixed relative translational energy of 0.62 eV that corresponds to the crossed beam experiments of Sonnenfroh *et al.*

COH_2^+ is a critical intermediate here, in agreement with work by Ishikawa *et al.* and in contrast with the interpretation of the crossed-beam experiments of Sonnenfroh *et al.* Virtually all trajectories generate COH^+ but a significant proportion of the isoformyl cation is formed with enough vibrational energy to isomerize to HCO^+ . Results here are almost fully coincident with Ishikawa. This work suggests that the reason for the discrepancy in the relative translational energy dis-

tribution between the crossed beam experiments and the trajectory computations should be either tunnelling or the contribution from the excited states.

Further analysis by Flores *et al.*¹⁷ suggested that the first excited electronic state of COH_2^+ could be important in the generation of the formyl isomer which has been detected in crossed-beam experiments but not in quasiclassical trajectory computations. Later work indicated that tunnelling has little impact on $\text{COH}^+/\text{HCO}^+$ branching ratios.¹⁸ They showed that the lowest-lying excited state presents topological features which favor the production of HCO^+ . Ab-initio molecular dynamics simulation of the $\text{C}^+ + \text{H}_2\text{O}$ reaction by Yamamoto¹⁹ have reiterated many of the findings of Flores, Ishikawa and their co-workers.

Despite the perceived significance of this process, studies of carbon ion irradiation of water in the condensed phase have been quite limited. Strazzulla *et al.*²⁰ have used 30 keV $^{13}\text{C}^+$ ions to irradiate 1 μm thick water ice films at 16 K and 77 K. $^{13}\text{CO}_2$ was observed as the dominant product while a small quantity of ^{13}CO was observed only at higher ion fluences. Dawes *et al.*²¹ have irradiated water ice at 30 and 90 K using low energy 4 keV $^{13}\text{C}^+$ and $^{13}\text{C}^{2+}$ ions. $^{13}\text{CO}_2$ was observed as the only carbon bearing species formed. A later study²² using 2 keV ions reiterated these findings.

To the best of our knowledge, the only theoretical study of C^+ irradiation of water in the condensed-phase is previous work by one of us,²³ where projectile energies between 0.175 keV and 4 keV were considered, and the sample was a liquid water slab at 300 K. At the lowest energies complete stopping of C^+ was observed, with the formation of new chemical species like H_2O_2 and $\text{C}(\text{OH})_2^+$.

The aim of the present study is to simulate computationally the dynamics of irradiation of amorphous solid water by C^+ ions at very low temperatures, as a prototype for the interaction of C^+ with planetary and interstellar ices. We are particularly interested in identifying which products emerge depending on conditions such as the kinetic energy of the carbon projectile and the geometrical aspects of the collision. In next Section we describe the computational approach, then we present the results of the simulations, and finally we summarize our conclusions.

Computational Details

We have studied the dynamics of irradiation of water-ice clusters with low-energy singly-charged carbon ions at 30 K using first-principles molecular dynamics (FPMD) simulations. The clusters have been sampled from an amorphous slab which has been supplied by Arasa *et al.*²⁴ This slab, which has been used in their studies of photodesorption in water-ice, has been prepared such that its structure closely resembles that of the compact amorphous ice obtained experimentally at 30 K.

For the purposes of this work it was deemed unnecessary to use the entire slab containing 360 water molecules. Instead, a 30-molecule sample was selected for use in our simulations, exactly as in our previous study with neutral C projectiles.²⁵ The molecules were extracted from the uppermost portion of the slab thus representing the surface of the ice. Prior to the irradiation computational experiments, the system was quenched at 30 K for 250 fs in order to obtain initial velocities for the water molecules. This was achieved via a canonical (fixed temperature) FPMD simulation using a canonical sampling through velocity rescaling (CSVR) thermostat.²⁶

Although the size of the cluster has been significantly reduced when compared with the initial slab, the water molecules still experience the full ice structure. One consequence of the limited size of this sample, however, is the increased tendency of the water molecules to evaporate during the lifetime of our simulations. Following the introduction of the energetic projectile the temperature of the system rises enormously. Impact by an 11 eV carbon ion will cause the temperature of the system to rise to approximately 85000 K while an average energy of roughly 0.25 eV is imparted to each water molecule. This effect would surely be reduced through use of an enlarged ice sample or a heat sink at the boundary of the cluster. It is, however, a genuine feature of the irradiation process, that the sample experiences a huge local temperature increase that favors chemical reactivity in the time scales studied in the present work.

All simulations were carried out using the ab initio module QUICKSTEP of the CP2K package.²⁷ The electronic structure was computed at the all-electron level, within density functional theory (DFT) using the Gaussian and augmented plane waves method (GAPW). Here the Kohn-Sham orbitals are expanded in a Gaussian basis set while the electrostatic (Hartree) potential is

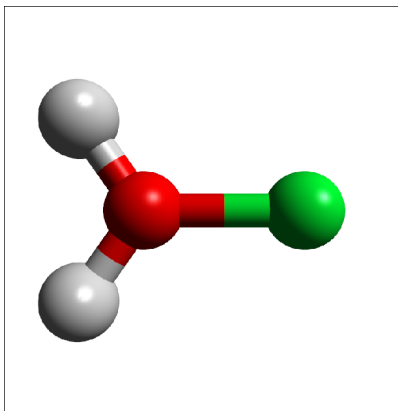


Figure 1: Optimized geometry for the C^+ -water complex. The C-O distance is given in Å for various theory levels.

computed by expressing the electronic density in plane waves (PW) augmented with atom-centered Gaussian functions. The latter are especially important within the framework of all-electron calculations because of the core orbitals, which would require PW with a very large energy. The augmentation approach allows for a significant reduction of the PW cutoff, to levels similar to those required in pseudopotential calculations.

After testing the quality of various approximations to exchange and correlation, we chose to use the hybrid PBE0 functional, which includes a Hartree-Fock exchange contribution combined with the Perdew-Burke-Ernzerhof (PBE) semi-local exchange-correlation term.²⁸ The 6-311G** basis set was selected as a good compromise between accuracy and computational efficiency. With this choice, basis set superposition errors are smaller than 3 %. The PBE0 functional was chosen based on the comparison of binding energies,

$$E_b = -[E(COH_2^+) - E(C^+) - E(H_2O)] \quad (4)$$

for the C^+ -water complex, see 1, against quantum chemical calculations at the MP2 and CCSD(T) level. The results of these calculations are reported in 1. These computations were carried out using the NWChem package.²⁹ The geometry of the complex was confirmed following extensive optimization calculations performed at the MP2/aug-cc-pVTZ level.

The calculated binding energies depend on the theory level, with Hartree-Fock and PBE at

Table 1: Calculated binding energies and COH_2^+ bond lengths for the C^+ -water complex.

Theory Level	Basis set	Binding energy (eV)	C-O bond length (Å)
HF	6-311G**	3.40	1.39
PBE	TZVP	4.60	1.40
PBE0	TZVP	4.38	1.39
MP2	aug-cc-pVTZ	4.02	1.37
CCSD(T)	aug-cc-pVTZ	3.96	1.38

the two extremes, respectively under- and over-binding. The binding energies produced by PBE0, MP2 and CCSD(T) are all approximately within 10 % of each other – PBE0 is within 10.6 % of CCSD(T).

Notice the significant binding energy difference with respect to the neutral complex, examined in our previous work,²⁵ where the theory level was much more relevant. Analysis of the electronic density reveals that the carbon ion actually makes a chemical bond with the water molecule. The C-O distance of 1.39 Å is significantly longer than the 1.13 Å in the CO molecule, but this is not surprising since the latter is a triple bond while in COH_2^+ we have a situation closer to a single bond. This is similar to the neutral COH_2 species which we previously reported,²⁵ where the C-O bond was 0.05 Å longer due to the additional electron. A consequence of the formation of this chemical bond is that the O-H bonds in the water molecule are weakened – elongating from 0.96 to 0.99 Å –, thus facilitating proton transfer from COH_2^+ to the neighboring water molecules in the condensed phase.

In respect of hydrogen bonds, it is well-documented that PBE0, due to the dominance of electrostatics, renders the geometries and energetics quite well in comparison to higher-level calculations and dispersion-corrected functionals.³⁰ As a check, equilibration of the cluster was repeated with the inclusion of Grimme’s semi-empirical van der Waals interaction.³¹ Comparison of the O-O distances for each cluster indicates that no significant changes result from the addition of these dispersion forces. To better assess the effect of the missing dispersion in PBE0, a trajectory in which COH^\bullet forms was repeated with the inclusion of the van der Waals interaction. There was no major change to the outcome of this trajectory, which once again produced COH^\bullet (see supporting information).

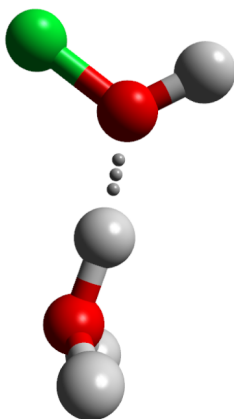


Figure 2: Optimized geometry for the $\text{COH}\cdots\text{H}_3\text{O}^+$ complex. Dots indicate the hydrogen bond, with an $\text{O}\cdots\text{H}$ distance of 1.47 Å at the PBE0/TZVP level (1.50 Å at the MP2/aug-cc-pVTZ level). The binding energy is approximately 0.7 eV.

As a further test of the PBE0 functional we have compared the binding energy and hydrogen bond length for $\text{COH}\cdots\text{H}_3\text{O}^+$ complex (see 2) at the PBE0/TZVP and MP2/aug-cc-pVTZ level. This entity appears in practically all the FPMD simulations. The calculated binding energies are 0.69 eV (PBE0) and 0.73 eV (MP2), while the bond lengths measure 1.47 Å and 1.50 Å. We now find that the disparity between the levels of theory which had been observed earlier (see 1) is greatly reduced. It is also apparent from our calculations that there is no barrier to the formation of $\text{COH}\cdots\text{H}_3\text{O}^+$ in the gas-phase reaction



We believe this level of agreement is sufficient to describe, with reasonable accuracy, collisions where the C^+ ion binds to a water molecule. Although MP2 generally outperforms PBE0, the much higher computational expense incurred through its use is, in our opinion, not justifiable, while this type of simulations are simply not viable at the CCSD(T) level of theory.

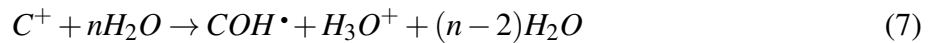
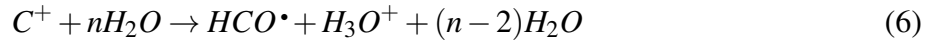
The configuration of water molecules obtained following the completion of the canonical FPMD run was used as a starting point for each of the subsequent simulations. Initial kinetic energies of 1.7 eV and 11 eV were chosen for the carbon projectile. Those two energies were

selected as representative of two distinct situations. At 11 eV the projectile has the energy required to dissociate a water molecule (5.1 eV), while at 1.7 eV water dissociation must proceed through other, more complex channels. For each of these energies 15 microcanonical (total energy of the system is fixed) runs were completed where, in each case, the carbon projectile had a different starting position and/or direction of approach. We also looked at higher-energy projectile, but these pass right through the cluster without stopping, thus not generating new chemical species. Clearly, 30 simulations are not statistically significant in order to extract information about probabilities and cross sections. However, the goal of the present work is to identify collision channels rather than to estimate cross sections.

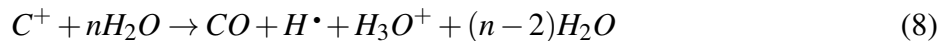
Results

Reported here are the products that result from the reactions following relatively low-energy collisions between the carbon ion and water-ice clusters. Our simulations have produced the following carbon bearing species:

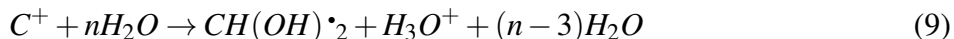
Formyl and isoformyl radicals:



carbon monoxide:



and the dihydroxymethyl radical:



where n is the number of water molecules, in this case $n = 30$.

In all cases, in the aftermaths of the collision, the positive charge of the system is held by a proton that forms a hydronium ion in the condensed-phase environment.

Isoformyl Formation

7 describes the production of the isoformyl radical ($COH\cdot$). This molecule appears as the final product in a third of our simulations. We find that the formation of $COH\cdot$ radicals is favored to a larger extent at lower energies.

The reaction mechanism for the formation of $COH\cdot$ has been identified. The sequence of steps for such a trajectory are depicted in 3.

As the carbon ion approaches the cluster it makes a bond with the oxygen of a water molecule upon impact (*b*). It has been found that at this point the reaction may proceed in either one of two ways. Depending on the energy of the carbon ion and its angle of impact, the $COH\cdot$ radical may be produced directly or through an intermediate. In the direct, “knock-out”, mechanism the carbon ion simply ejects a proton from the water molecule, which then goes on to form a hydronium ion, H_3O^+ , in the cluster. This is a relatively rapid process and occurs when the C^+ projectile is more energetic. Shown in 3(*b*) is the formation of an intermediate, COH_2^+ . When compared with the “knock-out” mechanism (not shown), the carbon ion is bonded to the water molecule for significantly longer (about 80 fs) before a proton detaches.

As the reaction proceeds we see that as the carbon ion forms a bond with the water molecule, it weakens one of its OH bonds eventually leading to the detachment of a proton (*c*). This proton subsequently joins a nearby water to form a positively charged hydronium (*d*), leaving the neutral

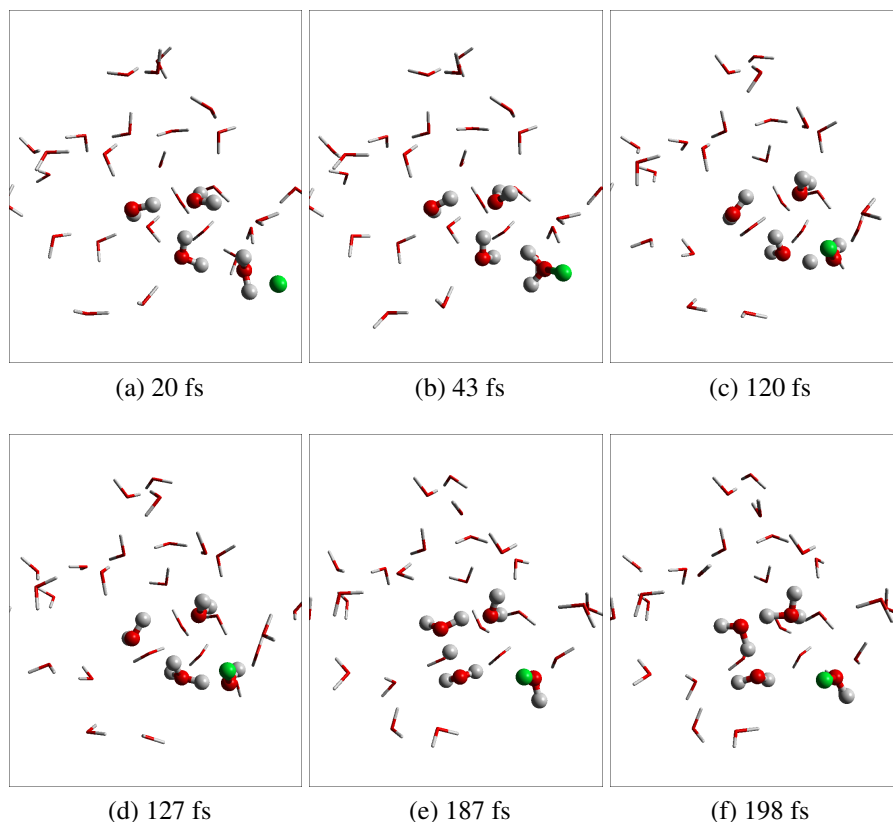


Figure 3: A selection of frames from a trajectory in which the isoformyl radical (COH^\bullet) forms. The atoms/molecules which participate directly in the reaction have been represented by *spheres*. The remaining water molecules are shown as *tubes*.

COH^\bullet radical. Following this it was possible to observe proton transfer from hydronium to neighboring water molecules within the cluster, (e) and (f). This continues until a stable arrangement is found, after dissipating the necessary amount of kinetic energy. H_3O^+ is a dynamical species at room temperature, with the proton diffusing via the Grotthuss mechanism.^{32,33} However, at the low temperatures considered here, the crucial step of reorientation of water molecules to create the appropriate environment for proton transfer is kinetically hindered. Therefore, the proton transfer stops after a few steps. The kinetic energy of the projectile is transferred to the water molecules, which occasionally evaporate from the cluster. At this point the simulation becomes unrealistic because a significant part of this energy should be dissipated through the ice environment, which is absent in the cluster geometry. Hence, we stop the simulation at this stage.

Formyl Formation

In agreement with the literature pertaining to gas phase MD calculations, we have found that production of the formyl (HCO) species does not occur as readily as isoformyl. However, it has been observed that under the conditions of our simulations HCO^\bullet creation is more common here than in the gas phase. Notice, however, that in the condensed phase we observe neutral radicals instead of cations (as in the gas phase). This may be due to the moderating presence of the ice environment, which solvates and screens the positively charged protons. In the gas phase dissociation proceeds by losing a hydrogen atom instead of a proton.

6 describes the production of the HCO^\bullet radical. The molecule was found as the final product in five of the trajectories. A tendency to favor low-energy trajectories was also expressed here.

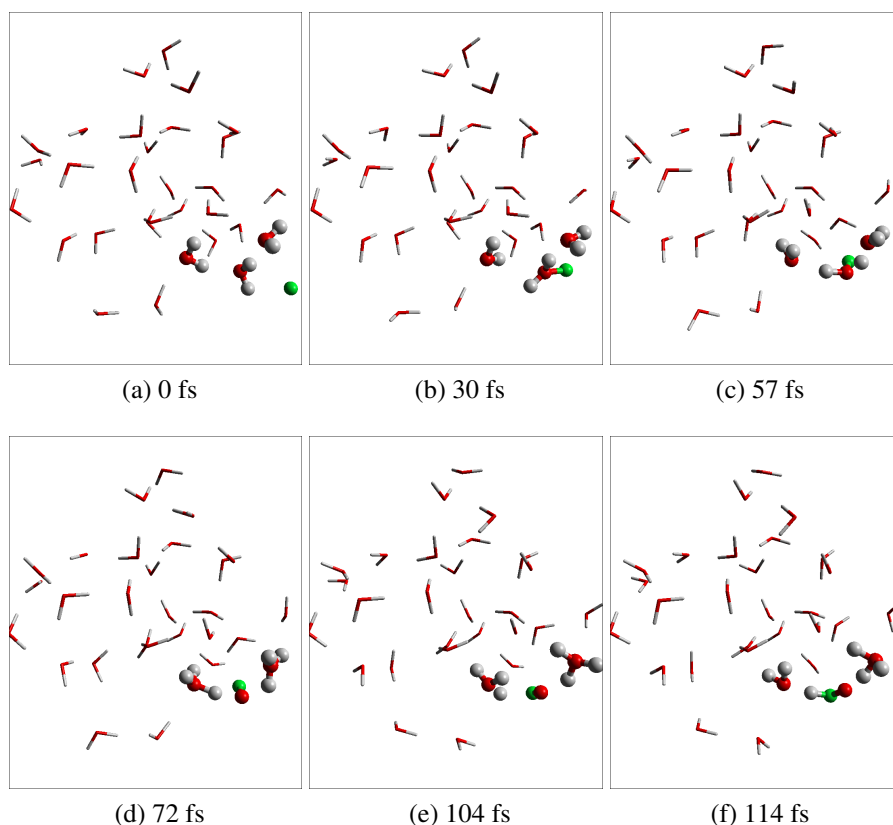


Figure 4: A selection of frames from a trajectory in which the formyl radical (HCO^\bullet) forms. The atoms/molecules which participate directly in the reaction have been represented by *spheres*. The remaining water molecules are shown as *tubes*.

4 shows the most common route to the formation of HCO^\bullet . The process begins similarly to that seen in the formation of COH^\bullet . In this case two protons detach following the initial impact of the carbon ion (*d*). A CO^- radical is left temporarily surrounded by a pair of hydronium molecules. Subsequently, a proton from one of the hydronium molecules rebinds to the carbon. The neutral HCO^\bullet radical is thus produced, leaving one remaining positively charged hydronium, H_3O^+ .

On one occasion we also observed HCO^\bullet production via formation of an HCOH^+ intermediate (see 5), as described by Ishikawa for the gas phase.¹⁴ Following the initial formation of the COH^\bullet radical (*b*) the molecule repositions itself allowing for the attachment of a proton from a neighboring hydronium species to the carbon atom (*d*). A relatively long period of time (~ 50 fs) now elapses in which the hydroxymethylene ion reorients enabling the transfer of the oxygen-bonded proton to a water molecule (*e*).

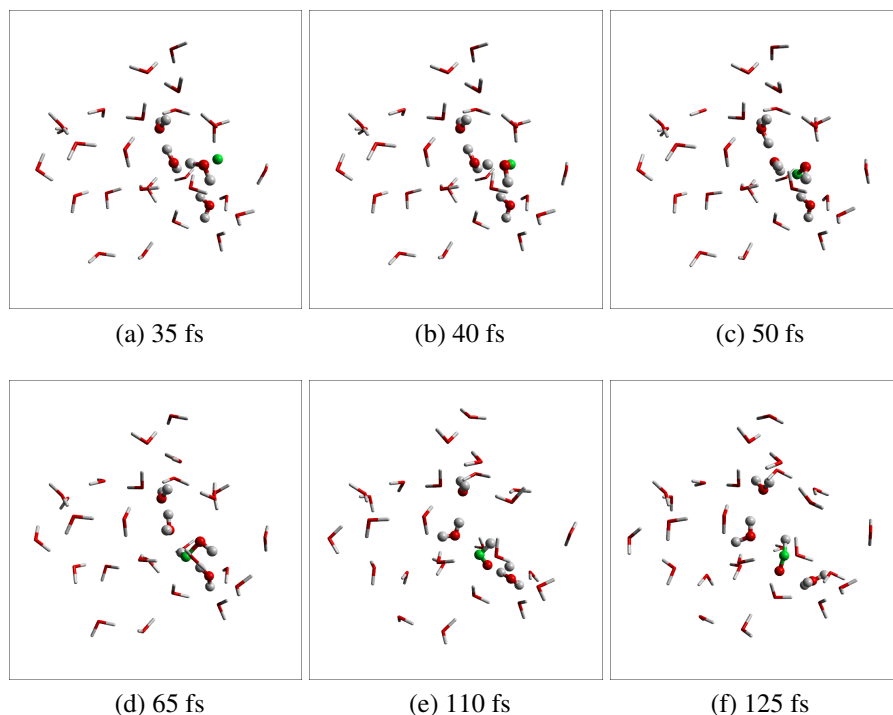
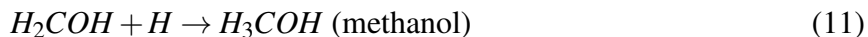


Figure 5: A selection of frames from a trajectory in which the formyl radical (HCO^\bullet) forms via HCOH^+ . The atoms/molecules which participate directly in the reaction have been represented by *spheres*. The remaining water molecules are shown as *tubes*.

Carbon Monoxide Formation

8 describes the production of carbon monoxide, CO, which formed in 40 % of our simulations. Trajectories in which the carbon ion had the higher kinetic energy of 11 eV were favored for CO production by approximately a factor of 2 with respect to those at the lower energy. The mechanism for its formation is not unique. CO is created when a hydrogen atom detaches from the newly created COH• or HCO• radicals, usually COH•. This (neutral) hydrogen atom will often evaporate from the ice cluster, as its interaction with water molecules is very weak. In fact, our calculations show that the H–H₂O binding energy is of the order of a few meV. In a larger sample of ice molecules, this hydrogen atom may act as a secondary projectile. Such low-energy hydrogens generally react with other radicals saturating their valence, as shown in the following reactions:



that are of crucial relevance in the formation of methanol on icy grains. We will look at these reactions in a forthcoming paper.

Dihydroxymethyl Formation

A rare occurrence in these simulations is the creation of the dihydroxymethyl radical CH(OH)₂•, which is a relatively complex species involving a C atom and two water molecules. Of the 30 trajectories simulated, three produced the CH(OH)₂• species. In all cases the carbon ion had an initial energy of 1.7 eV with CH(OH)₂• forming in the same manner each time, as depicted in 6.

In this trajectory the carbon ion binds to a pair of water molecules through the oxygens. These, in turn, form hydrogen bonds with neighboring waters (*b*). Subsequently, a proton is removed from one of the waters in a similar manner to that seen in our previous trajectories. What remains is a carbon-water complex which now has a hydroxyl group (OH[−]) bound to the carbon and a

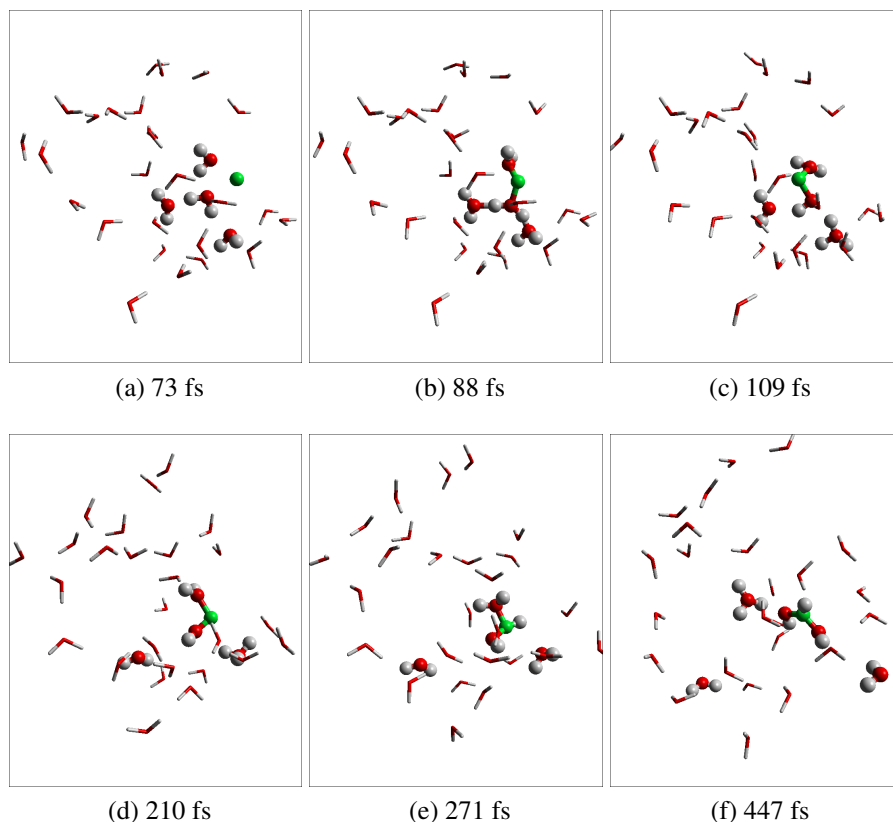


Figure 6: A selection of frames from a trajectory in which the dihydroxymethyl radical ($\text{CH}(\text{OH})_2^\bullet$) forms. The atoms/molecules which participate directly in the reaction have been represented by *spheres*. The remaining water molecules are shown as *tubes*.

nearby hydronium (*c*). This carbon-bearing species now repositions itself over a time period of approximately 150 fs, making the carbon available to the hydronium (*d*). The carbon then accepts a proton from the hydronium ion (*e*). In the remainder of the simulation we observe that the carbon-bearing molecule loses a proton once more, leaving the neutral dihydroxymethyl radical and a hydronium ion as final products.

Dihydroxymethyl is a precursor of more stable organic molecules such as formic acid (HCOOH), which is achieved by the loss of a hydrogen atom. The addition of a hydrogen atom, which is an abundant species in the ISM, may produce methanediol ($\text{CH}_2(\text{OH})_2$) which participates in the synthesis of simple sugars. Both formic acid and methanediol are predicted to form on grain surfaces and are of prebiotic significance.³⁴ Dihydroxymethyl was not proposed before because gas-phase work involved a single water molecule. These condensed-phase simulations highlight the possi-

bility of near-neighbor interactions which are not a feature of gas-phase chemistry and provide a less complex path to chemical complexity. Some of these reactions have been observed in previous work with higher-energy C^+ projectiles interacting with water slabs²³ and are consistent with gas-phase work.

Concluding remarks

We have investigated the interaction of low-energy singly-charged carbon ions (C^+) with amorphous solid water clusters at 30 K via first-principles molecular dynamics simulations. We have selected initial projectile energies of 11 eV and 1.7 eV. These energies are attained after the (generally) more energetic projectiles ($E \sim 2$ keV)²¹ have travelled through the medium losing energy via inelastic collisions, as shown in a previous publication.²³ At such low energies the carbon ions can participate in chemical reactions and generate new organic chemical species. At the higher energy of 11 eV the kinetic energy of the carbon is large enough to dissociate a water molecule (5.1 eV) by impact alone, but not at the lower energy. Along their way, the C^+ ions can also capture electrons produced by ionization thus becoming neutral carbon atoms. In that case, the results of our previous study²⁵ apply.

The dominant products are the isoformyl radical (COH^\bullet) and carbon monoxide (CO). COH^\bullet formation is favored slightly among trajectories where the C^+ projectile has an initial energy of 1.7 eV. CO is produced more abundantly with 11 eV projectiles. Depending on the energy of impact of the C^+ projectile, COH^\bullet will be created via either a direct, “knock-out” mechanism, or through a COH_2^+ intermediate. In the direct mechanism the carbon ion will simply eject a proton from a water in a relatively rapid reaction. This is more likely to occur at higher energies. The formation of the COH_2^+ intermediate occurs on a longer timescale. In each case the departing proton will be transferred among the water molecules of the cluster via a Grotthuss mechanism^{32,33} to form a hydronium ion. Carbon monoxide, the other major product of these reactions, is most commonly produced by the subsequent dissociation of COH^\bullet into $CO + H^\bullet$, with the hydrogen atom becoming

a secondary projectile that can react with other species in the sample, or simply evaporate.

A minor product of this reaction is the formyl radical ($\text{HCO}\cdot$). This is formed most commonly following an impact of the carbon ion with a water which strips it of its hydrogens causing the creation of two hydronium species and CO^- . A proton then returns to the remaining carbon monoxide anion and attaches at the site of the carbon atom. $\text{HCO}\cdot$ has also been produced via a hydroxymethylene intermediate. We observe more frequent production of the $\text{HCO}\cdot$ radical here than in similar gas phase reactions. The availability of additional water molecules in the cluster allows for alternative routes to $\text{HCO}\cdot$ formation.

If we compare this work with our previous study²⁵ we see that formyl and isoformyl radicals along with carbon monoxide appear as products in both, although in the neutral case they are accompanied by $\text{H}\cdot$ rather than the hydronium ions observed here. What we do not observe, however, is the hydroxymethylene radical which features prominently in our previous work and in the work of others who have studied the interaction of C with water.^{35–37}

An intriguing aspect is that we do not observe the formation of CO_2 as in experiments involving amorphous solid water, although the dihydroxymethyl radical may be a precursor of CO_2 on a longer timescale. Another possibility is that the $\text{COH}\cdot$ reacts with an oxygen atom that has been produced by a higher energy projectile fully dissociating a water molecule, as observed in earlier work.²³ Yet another possibility is that the C^+ captures one electron in an excited state when approaching the sample at higher energy. This leaves H_2O^+ , which dissociates as $\text{H}_2\text{O}^+ \rightarrow \text{OH}\cdot + \text{H}^+$. The $\text{OH}\cdot$ radical may then react with CO produced from a neutral carbon and water collision, as described in our previous publication,²⁵ leading to $\text{CO} + \text{OH}\cdot \rightarrow \text{CO}_2 + \text{H}\cdot$. These are interesting avenues to explore in the future.

Acknowledgement

Astrophysics at QUB is supported by a grant from the STFC. EM was supported by DEL (Northern Ireland). The CP2K calculations were carried out at the HECToR facility supported by EPSRC grants EP/F037325/1 and EP/K013459/1, allocated to the UKCP consortium.

Supporting Information Available

Results obtained using a dispersion-corrected functional. This material is available free of charge via the Internet at <http://pubs.acs.org/>.

References

- (1) Dumas, G.; Vaupré, S.; Ceccarelli, C.; Hily-Blant, P.; Dubus, G.; Montmerle, T.; Gabici, S. Localized SiO Emission Triggered by the Passage of the W51C Supernova Remnant Shock. *Astrophys. J. Lett.* **2014**, 786, L24.
- (2) Dalgarno, A. Spiers Memorial Lecture. The Chemistry of Astronomical Environments. *J. Chem. Soc. Faraday Trans.* **1993**, 89, 2111–2117.
- (3) Herbst, E. The Chemistry of Interstellar Space. *Chem. Soc. Rev.* **2001**, 30, 168–176.
- (4) Lee, H. H.; Bettens, R. P. A.; Herbst, E. Fractional Abundances of Molecules in Dense Interstellar Clouds: A Compendium of Recent Model Results. *Astron. Astrophys. Suppl. Ser.* **1996**, 119, 111–114.
- (5) Bochsler, P. Abundances and Charge States of Particles in the Solar Wind. *Rev. Geophys.* **2000**, 38, 247–266.
- (6) Kempf, S.; Srama, R.; Postberg, F.; Burton, M.; Green, S. F.; Helfert, S.; Hillier, J. K.; McBride, N.; McDonnell, J. A. M.; Moragas-Klostermeyer, G.; Roy, M.; Grün, E. Composition of Saturnian Stream Particles. *Science* **2005**, 307, 1274–1276.
- (7) Schiff, H. I.; Bohme, D. K. An Ion-molecule Scheme for the Synthesis of Hydrocarbon-chain and Organonitrogen Molecules in Dense Interstellar Clouds. *Astrophys. J.* **1979**, 232, 740–746.
- (8) Herbst, E.; Adams, N. G.; Smith, D. Laboratory Measurements of Ion-molecule Reactions Pertaining to Interstellar Hydrocarbon Synthesis. *Astrophys. J.* **1983**, 269, 329–333.

- (9) Martinez, Jr., O.; Betts, N. B.; Villano, S. M.; Eyet, N.; Snow, T. P.; Bierbaum, V. M. Gas Phase Study of C⁺ Reactions of Interstellar Relevance. *Astrophys. J.* **2008**, *686*, 1486–1492.
- (10) Maergoiz, A. I.; Nikitin, E. E.; Troe, J. Capture of Asymmetric Top Dipolar Molecules by Ions: Rate Constants for Capture of H₂O, HDO, and D₂O by Arbitrary Ions. *Int. J. Mass Spectrom.* **2009**, *280*, 42–49.
- (11) Herbst, E.; van Dishoeck, E. F. Complex Organic Interstellar Molecules. *Annu. Rev. Astron. Astrophys.* **2009**, *47*, 427–480.
- (12) McCord, T. B.; Carlson, R. W.; Smythe, W. D.; Hansen, G. B.; Clark, R. N.; Hibbitts, C. A.; Fanale, F. P.; Granahan, J. C.; Segura, M.; Matson, D. L.; Johnson, T. V.; Martin, P. D. Organics and Other Molecules in the Surfaces of Callisto and Ganymede. *Science* **1997**, *278*, 271–275.
- (13) Sonnenfroh, D. M.; Curtis, R. A.; Farrar, J. M. Collision Complex Formation in the Reaction of C⁺ with H₂O. *J. Chem. Phys.* **1985**, *83*, 3958–3964.
- (14) Ishikawa, Y.; Binning, Jr., R. C.; Ikegami, T. Direct Ab Initio Molecular Dynamics Study of C⁺ + H₂O. *Chem. Phys. Lett.* **2001**, *343*, 413–419.
- (15) Ishikawa, Y.; Ikegami, T.; Binning, Jr., R. C. Direct Ab Initio Molecular Dynamics Study of C⁺ + H₂O: Angular Distribution of Products and Distribution of Product Kinetic Energies. *Chem. Phys. Lett.* **2003**, *370*, 490–495.
- (16) Flores, J. R. Quasiclassical Trajectories on a Finite Element Density Functional Potential Energy Surface: The C⁺ + H₂O Reaction Revisited. *J. Chem. Phys.* **2006**, *125*, 164309.
- (17) Flores, J. R.; González, A. B. The Role of the Excited Electronic States in the C⁺ + H₂O Reaction. *J. Chem. Phys.* **2008**, *128*, 144310.
- (18) Flores, J. R. Further Quasi-classical Trajectory Studies on the C⁺ + H₂O Reaction. *Mol. Simulat.* **2009**, *35*, 325–333.

- (19) Yamamoto, J. Ab Initio Molecular Dynamics Simulation on $\text{H}_2\text{O} + \text{C}^+$ Reaction. *J. Mol. Struct. (Theochem)* **2010**, 957, 55–60.
- (20) Strazzulla, G.; Leto, G.; Gomis, O.; Satorre, M. A. Implantation of Carbon and Nitrogen Ions in Water Ice. *Icarus* **2003**, 164, 163–169.
- (21) Dawes, A.; Hunniford, A.; Holtom, P. D.; Mukerji, R. J.; McCullough, R. W.; Mason, N. J. Low Energy $^{13}\text{C}^+$ and $^{13}\text{C}_2^+$ Ion Irradiation of Water Ice. *Phys. Chem. Chem. Phys.* **2007**, 9, 2886–93.
- (22) Hunniford, C. A.; Dawes, A.; Fulvio, D.; Sivaraman, B.; Merrigan, T. L.; McCullough, R. W.; Mason, N. J.; Palumbo, M. E. Irradiation of Water Ices by 2 keV Carbon Ions. *J. Phys.: Conf. Ser.* **2009**, 163, 012078.
- (23) Kohanoff, J. J.; Artacho, E. First-Principles Molecular Dynamics Simulations of the Interaction of Ionic Projectiles with Liquid Water and Ice. *AIP Conf. Proc.* **2008**, 1080, 78–87.
- (24) Arasa, C.; Andersson, S.; Cuppen, H. M.; van Dishoeck, E. F.; Kroes, G. J. Molecular Dynamics Simulations of the Ice Temperature Dependence of Water Ice Photodesorption. *J. Chem. Phys.* **2010**, 132, 184510.
- (25) McBride, E. J.; Millar, T. J.; Kohanoff, J. J. Organic Synthesis in the Interstellar Medium by Low-Energy Carbon Irradiation. *J. Phys. Chem. A* **2013**, 117, 9666–9672.
- (26) Bussi, G.; Donadio, D.; Parrinello, M. Canonical Sampling Through Velocity Rescaling. *J. Chem. Phys.* **2007**, 126, 014101.
- (27) VandeVondele, J.; Krack, M.; Mohamed, F.; Parrinello, M.; Chassaing, T.; Hutter, J. Quickstep: Fast and Accurate Density Functional Calculations Using a Mixed Gaussian and Plane Waves Approach. *Comput. Phys. Commun.* **2005**, 167, 103–128.
- (28) Perdew, J. P.; Burke, K.; Ernzerhof, M. Generalized Gradient Approximation Made Simple. *Phys. Rev. Lett.* **1996**, 77, 3865–3868.

- (29) Valiev, M.; Bylaska, E. J.; Govind, N.; Kowalski, K.; Straatsma, T. P.; Van Dam, H. J. J.; Wang, D.; Nieplocha, J.; Apra, E.; Windus, T. L.; et al., NWChem: A Comprehensive and Scalable Open-Source Solution for Large Scale Molecular Simulations. *Comput. Phys. Commun.* **2010**, *181*, 1477–1489.
- (30) Thanthiriwatte, K. S.; Hohenstein, E. G.; Burns, L. A.; Sherrill, C. D. Assessment of the Performance of DFT and DFT-D Methods for Describing Distance Dependence of Hydrogen-bonded Interactions. *J. Chem. Theory Comput.* **2011**, *7*, 88–96.
- (31) Grimme, S. Semiempirical GGA-type density functional constructed with a long-range dispersion correction. *Journal of Computational Chemistry* **2006**, *27*, 1787–1799.
- (32) de Grotthuss, C. J. T. Sur la décomposition de l'eau et des corps qu'elle tient en dissolution à l'aide de l'électricité galvanique. *Ann. Chim.* **1806**, *58*, 54–73.
- (33) Agmon, N. The Grotthuss Mechanism. *Chem. Phys. Lett.* **1995**, *244*, 456–462.
- (34) Garrod, R. T.; Weaver, S. L. W.; Herbst, E. Complex Chemistry in Star-forming Regions: An Expanded Gas-grain Warm-up Chemical Model. *Astrophys. J.* **2008**, *682*, 283–302.
- (35) Ahmed, S. N.; McKee, M. L.; Shevlin, P. B. An Experimental and Ab Initio Study of the Addition of Atomic Carbon to Water. *J. Am. Chem. Soc.* **1983**, *105*, 3942–3947.
- (36) Schreiner, P. R.; Reisenauer, H. P. The "Non-Reaction" of Ground-State Triplet Carbon Atoms with Water Revisited. *ChemPhysChem* **2006**, *7*, 880–885.
- (37) Ozkan, I.; Dede, Y. Reactions of 1S, 1D, and 3P Carbon Atoms with Water. Oxygen Abstraction and Intermolecular Formaldehyde Generation Mechanisms; An MCSCF Study. *Int. J. Quant. Chem* **2012**, *112*, 1165–1184.

